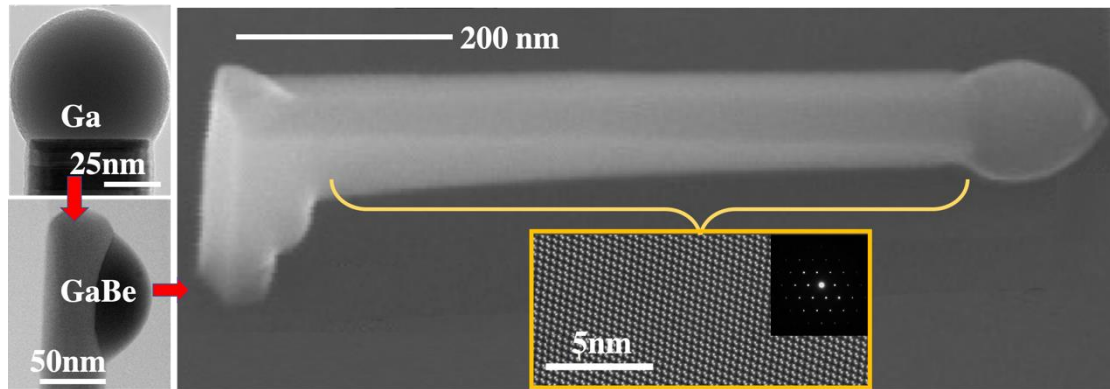# Droplet Manipulation and Horizontal Growth of High-Quality Self-Catalysed GaAsP Nanowires

Droplet Manipulation and Horizontal Growth of High-Quality Self-Catalysed GaAsP Nanowires

Yunyan Zhang,[a*] Ana M. Sanchez,[b] Martin Aagesen,[c] H. Aruni Fonseka,[b] Suguo Huo,[d] and Huiyun Liu [a]

[a] Department of Electronic and Electrical Engineering, University College London, London WC1E 7JE, United Kingdom

[b] Department of Physics, University of Warwick, Coventry CV4 7AL, United Kingdom

[c] Center for Quantum Devices, Niels Bohr Institute, University of Copenhagen, Universitetsparken 5, 2100 Copenhagen, Denmark

[d] London Centre for Nanotechnology, University College London, London WC1H 0AH, United Kingdom

Abstract: Self-catalyzed horizontal nanowires (NWs) can greatly simplify the CMOS integration processing compared with the regular vertical counterparts. However, self-catalysed growth mode poses challenges in manipulating the droplets to produce single-crystalline horizontal NWs with a uniform diameter. Here, we demonstrated a novel method to manipulate the droplet through altering the droplet surface energy. Ga-droplet was successfully moved from top to sidewalls in GaAsP NWs by introducing Be and lowering the surface energy, and pinned at the tip despite the absence of planar defects. This can switch the <111> growth direction, with a successful rate of 100%, from vertical to horizontal through the assistance of few sparse twins. The produced NWs tend to be bounded by low energy facets, which leads to the self-catalysed growth

of horizontal NWs with a greatly improved diameter uniformity along the axis. Besides, the lowered surface energy can effectively suppress the wurtzite nucleation, producing pure zinc blende single-crystalline horizontal NWs. This study establishes an essential step toward the efficient integration of NWs into CMOS compatible devices.

Key words: horizontal nanowires, self-catalyzed droplet, surface energy.

Introduction

Nanowires (NWs) have novel mechanical, optical and electronic properties that are not seen in the thin-film counterparts [1−5] and they continue generating wide research interests [6−13]. The surface of NWs can have atomic-level smoothness that cannot be achieved by traditional etching methods, which can greatly reduce the surface roughness-induced carrier scattering [14]. When made of III-V materials, NWs also have greatly enhanced carrier mobility that can be 4~60 times higher than that of Si. All these are essential for making high-speed electronics. It has been shown that III-V NWs can easily outperform the group-IV material counterparts in making logic devices [15]. Besides, the III-V logic devices can have a much higher operation temperature compared with the group-IV ones. With traditional thin-film growth methods, there are huge challenges in integrating high-quality III-V devices onto Si platform due to the large lattice and thermal property mis-matches between them. Although the traditional bonding method can achieve small-number device integration, it cannot satisfy the fabrication of high-density integrated circuits that requires massive device integration. NWs, with a nanoscale dimension, can efficiently relax more strain elastically than thin

films, opening a good solution to monolithic integration of a large number of high-quality III-V devices onto the Si platform in a cost-effective way [16,17]. Although Si (111) substrates are commonly used due to the simplicity in the NW growth, there is no problem to grow vertical and horizontal NWs on (100) substrates [18-21]. Thus, III-V NWs are very promising for future CMOS technologies, such as MESFETs, MOSFETs, and HEMTs [22-24].

So far, the growth technique for free-standing NWs are well developed, especially the regular vertical ones [25,26]. Although devices based on those NWs have been fabricated [27], horizontal planar NWs are preferred for compatibility with the widely-used planar processing technique. Great effort has been devoted to horizontal NWs from groups worldwide [28-35], such as Li group [36], with significant breakthroughs in controlling the parameters of these horizontal NWs, such as length, diameter, direction and uniformity [36,37].

Vapor-liquid-solid (VLS) mechanism has been the approach of choice to grow horizontal III-V NWs [38], which utilizes a nano-size liquid droplet to transport growth material into the liquid-solid growth interface. This growth, initially used for growing vertical NWs, provides easier control of the growth direction compared to other growth modes based on droplet manipulation [39]. The growth environment for horizontal NWs is quite different from that of the vertical ones, such as source material impingement and the material diffusion from the substrate, affecting the effective III/V ratio. Due to the complexity of this type of growth, most of the research on horizontal NWs have been performed using foreign−metal−catalysed growth modes, especially

the Au [28,29,36,40]. The foreign−metal catalytic droplets are not consumed during the growth, making it easy to manipulate the droplet within a large growth parameter window [41,42]. However, most foreign metals have a number of drawbacks, which make them rather unpopular. For example, the Au can incorporate with a rather high concentration into the NWs, degrading greatly the device performance [43]; e.g. 10^{17}~10^{18}/cm^3 in the Au-catalysed GaAs and InAs NWs [44,45]. More seriously, Au has a high solid diffusivity, which can easily cause contamination to the exposed fabrication equipment, being extremely hard to remove. Au impurities can also form mid−gap energy states when incorporated into Si, affecting the device performance [43,45]. Therefore, the Au catalyzed NWs are incompatible with the Si-based IC industry.

The self-catalyzed growth mode is based on the use of the same group-III element both in the droplet and the NW, such as Ga droplet for GaAsP NWs [46]. Therefore, it does not cause any contamination from the catalytic droplet, unlike the foreign metal catalysed growth. However, the self-catalytic droplet is consumable during the growth and very sensitive to the growth environment. Slight fluctuation in the growth parameters can cause high-density of defect in the NW or even the growth failure [47]. Thus, the droplet manipulation is very difficult. Fontcuberta *et al*. developed a creative droplet manipulation method [48]. By annealing under the vacuum, they increased the droplet size by tip thermal decomposition and successfully removed the droplet from the NW top to the sidewalls. Koivusalo *et al*. [49] and Li *et al*. [31] used similar method to switch the growth direction of self-catalyzed GaAs NWs. So far, the self-catalyzed

horizontal NWs are still facing the crystal quality and/or the morphology issues that can largely degrade device performance and affect the integration quality. These NWs tend to have high density of stacking faults perpendicular to the NW axis or single twins along the entire NW axis [49]. Besides, these defects can generate new high-energy micro-facets on the NW surface [25] and promote significant parasitic shell growth, leading to beak-like shape [49]. Thus, more research is needed to achieve single crystalline horizontal NWs with a uniform diameter.

In this paper, we demonstrated a self-catalytic droplet manipulation method through surface energy alteration, which further leads to the growth of high-quality horizontal NWs. This study effectively solved the severe stacking-fault-formation problems and greatly alleviated the parasitic-shell-growth issues during the growth of self-catalyzed horizontal NWs [49].

Results and discussion

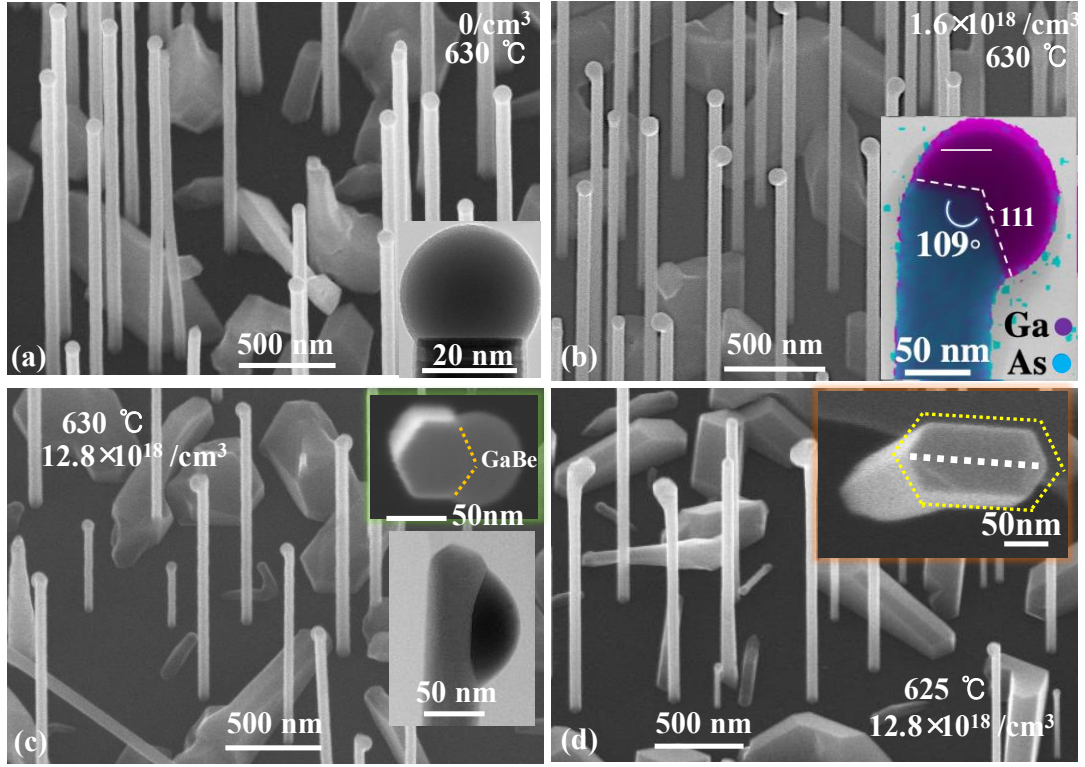*Droplet manipulation through changing surface energy*

Fig. 1. Scanning electron microscope image (SEM), low magnification TEM, and composition mapping images of GaAs NWs grown with various Be fluxes and temperatures. The nominal Be flux and growth temperature of (a) $0/cm^3$, 630 ℃, (b) $1.6×10^{18}/cm^3$, 630 ℃, (c)$1.28×10^{19}/cm^3$, 630 ℃, and (d) $1.28×10^{19}/cm^3$, 625 ℃. The insets in the images are the side or top views of the NW tip.

In droplet-catalyzed NW growth, the droplet location controls the NW growth direction. As can be seen in Fig. 1a and more clearly in the inset, the Ga droplet sits on the top of the GaAs NW with a flat interface. Here, the growth is along the NW axial direction. To switch the growth direction from axial (vertical) direction to side (horizontal) direction, the droplet needs to move from the top facet to the sidewalls. However, this is a challenging process since the monolayer-by-monolayer growth mode

favours the droplet to move along the axial direction due to lowest surface energy of the (111) (or WZ equivalent (0001)) facets. In order to break this preferential growth along the axial direction, *Be* flux was introduced during the growth, changing the Ga droplet composition into a Be containing droplet, Ga(Be). *Be* can effectively lower the surface energy of the Ga droplet and distort its shape [50,51].

This process can be described by the Young's equation [52], $cos\theta = (\gamma_{SG} - \gamma_{SL})/\gamma_{LG}$. Where the γ_{SG}, γ_{SL}, and γ_{LG} relate to the surface tensions between the three phases: solid, liquid and gas, and θ is the contact angle of a liquid droplet on a solid surface. The reduction of the surface tension γ_{LG} can lead to the reduction of θ and induce a partial wetting of Ga(Be) droplet on the side walls, which can be seen from the GaAs NWs grown with a Be flux equivalent to a nominal thin-film doping concentration of 1.6×10^{18}/cm^3 (Fig. 1b). The sidewall wetting can cause the generation of new (111) facets with an angle of 109º relative the top facet. Further increase the Be flux to 1.28×10^{19}/cm^3 during the growth, the greatly lowered surface energy can move the droplet completely to the sidewall (Fig. 1c).

The temperature is very critical for keeping the droplet unconsumed. The droplet on the side walls has a contact area which is ~2 times larger than when it is on the top facet, which implies a larger nucleation area (inset of Fig. 1c). A low droplet supersaturation environment is beneficial to prevent the fast solidification of this droplet. As shown in Fig. 1c, the droplet is still liquid after growth at 630 ℃. Lowering the growth temperature by 5 ℃, the droplet supersaturation with group-V materials increased and solidified quickly (Fig. 1d) [53]. Thus, manipulating the droplet at the

optimized NW growth temperature is suggested, as this is the easiest way to keep the droplet liquid.

To understand the droplet pinning site on the sidewalls, NW top view images were taken by SEM. Self-catalysed NWs have a hexagonal cross section bounded by six {110} facets and six <112> corner ridges [54,55], as can be observed in the inset of Fig. 1c. This image also reveals how the droplet prefers to straddle a <112> corner ridge and cover two {110} facets. Therefore, the droplet can be controlled to point to a <112> direction. The same phenomenon is also observed in NWs with a solidified droplet (Fig. 1d). The solidified droplet retains the hexagonal shape but it is elongated along the central <112> diagonal lines, confirming that the droplet straddle a corner ridge facing that <112> direction before solidified. So far, we have not found a solid evidence about if the droplet prefers any of the six <112> corners (Supporting information Fig. S1). A ring-shaped contact structure can easily solve this random corner issue (Supporting information Fig. S2), but developing a novel growth technique to achieve pre-defined direction control can still be very helpful for the device contact fabrication.
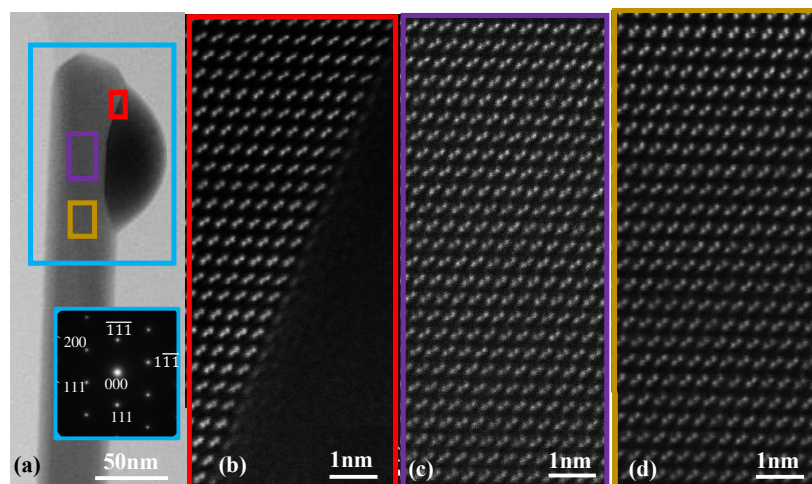
Pinning of droplets at the tip

Fig. 2. Crystal structure of droplet-displaced NWs. (a) Representative GaAs NW tip with an unconsumed droplet on the sidewalls. The inset corresponds to the selected-area electron diffraction (SAED) pattern in the blue square. (b)~(d) atomic-resolution annular dark field (ADF) images of different areas in the GaAs tip in (a).

Fig. 1c shows that although the droplets have been displaced to the sidewalls, they are still at the tip part of NWs. Previous studies have associated this pinning at the tip to the presence of stacking faults in that region, preventing it to slide along the NW [30, 56]. Further investigations on the crystal structure of NWs with the droplet displaced from the top (Fig. 2a) was carried out by (Scanning) Transmission electron microscopy, (S)TEM. Fig. 2b, c and d, revealed GaAs zinc blende (ZB) without the stacking faults and further confirmed by the SAED pattern (inset in Fig. 2a). Therefore, although the Ga(Be) droplet in GaAs NWs move towards the sidewall, it remains NW tip area, without sliding any further along that sidewall.

The high Be flux effectively lowers the surface energy of the Ga droplet. As we observed there, the droplet contact angle was decreased from >90° to <90° when the Be flux increased (Fig. 1a, b, and Fig. 2a) [57,58]. The droplet adhesion to the NWs increases with the reduction of the surface energy/tension and hence the contact angle [59,60]. Besides, the reduction of contact angle also gives the droplet a larger contact area with the sidewalls, which can have more adhesive bonds with the NW and hence provide a stronger force to "holds/embraces" NW, preventing it sliding along the length. Therefore, the Ga(Be) alloy droplet can pin itself to the tip of NWs and does not need the assistance of stacking faults to anchor the position.
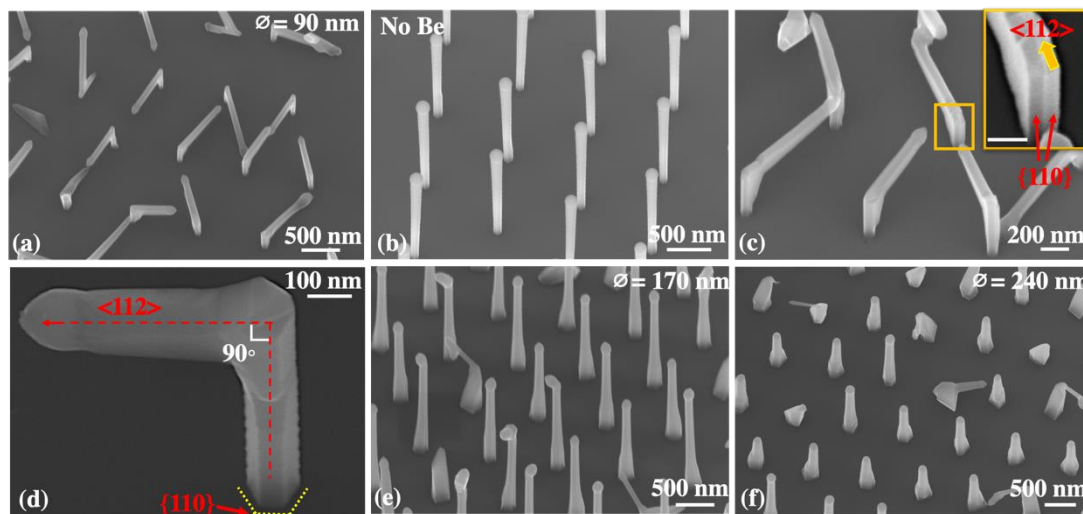
Growth of horizontal NWs

Fig. 3. SEM images of GaAs$_{0.8}$P$_{0.2}$ NWs grown on patterned Si substrates. All the growth parameters were kept the same except the Be fluxes and patterned hole size. (a) (c) and (d) L-shaped NWs grown with a Be flux equivalent to a nominal doping concentration of 1.5×10^{17} /cm^3 at the first 15 mins and then with 6×10^{17} /cm^3 for the rest 30 mins. The inset in (c) is a zoom in image of the yellow square area. Scale bar 100 nm. (b) NWs grown without a Be flux. (e) and (f) NWs with different diameters marked in the image grown under the same condition with (a).

With the droplet placed on the sidewalls of a NW tip, a new equilibrium conditions must be established for the catalysed VLS growth to continue in a direction 90° relative to the axial NW direction. To achieve this, patterned substrates are used in NW growth, on which the regular patterned hole pitch can provide similar growth environment for each NW and avoid uneven interaction between wires what commonly occurs during the growth on un-patterned substrates. Initial NW growth started with a low Be flux, i.e. an equivalent nominal doping concentration of 1.5×10^{17} /cm^3, during the first 15

mins. Later the doping concentration was increased 4 times, up to 6×10^{17} /cm^3. This process generated L-shaped NWs with 90±15 nm in diameter, as can be seen in Fig. 3a. The initial segment grown first of most NWs is in vertical direction, and the later-grown segment is straight and commonly in horizontal direction. For the growth that successfully produced the initial NW segment, a high yield of 100% has been achieved (Supporting information Fig. S3). One growth without Be flux were also performed as a comparison to Fig. 3a sample. The rest of parameters for the NW growth were kept the same. This growth conditions produced vertically standing NWs (Fig. 3b), without L-shaped ones. This comparison between different growth conditions confirmed that the high Be flux is responsible for the growth of L-shaped NWs, in accordance to the previous observation. It needs to be mentioned that the droplet is in an elongated shape which could be due to the lowered surface energy [61]. After the growth direction switch, the Be in the droplet can be depleted by incorporating into the NWs with the growth proceeding under no Be flux environment, and then Be-free horizontal segments can be grown.

This horizontal segment has its starting end bound by two {110} facets and elongates along the <112> direction as can be seen in Fig. 3c, similar to Fig. 1d. To check the angel between the vertical and horizontal segments, the sample was rotated to make the horizontal segment in parallel to the bottom line of Fig. 3d. This also makes the {110} facet (pointed by the red arrow), the one in the same plane as the horizontal segment, in parallel to the bottom line of Fig. 3d. Thus, a tilted front view was obtained. This view shows that the angle between the two segments is ~90°.

Another critical parameter to achieve L-shaped NWs is the NW diameter. The droplet movement from the top to sidewalls, by lowering surface energy, easily occurs in the NW with a smaller diameter. As can be seen in Fig. 3a, L-shaped NWs are formed for diameter of ~90 nm. For a lager diameter, i.e. 170 ± 18 nm, all the NWs stand vertically, with only few of them having a kinked head at the end of the growth, ie. when the NW diameter start getting reduced (Fig. 3e). When the diameter dramatically increased up to 240 ± 25 nm, none of the NWs developed into L shape (Fig. 3f). This variation with the NW diameter could be related to the dose difference required to reshape the droplet. Larger droplets require a larger amount of Be to reach an equal concentration as the smaller ones.
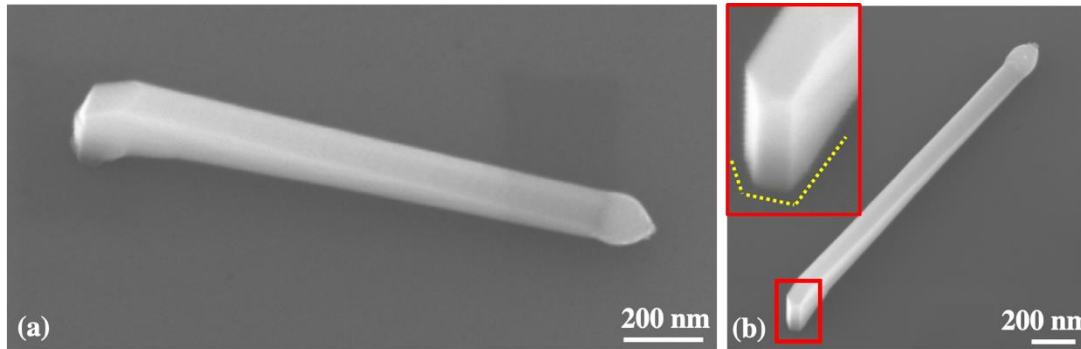

Fig. 4. SEM images of the doped horizontal $GaAs_{0.8}P_{0.2}$ NWs grown on the surface of Si substrates. The yellow dot lines in the inset of (b) are guiding to the eye about the {110} facets of the vertical NW segment.

As shown in Fig. 2a, the droplet is stable on the sidewalls at the tip of the NW. Therefore, the height of horizontal arm off the substrate can be adjusted by controlling the vertical segment, such as the ones shown in Fig. 3a. This provide a possible path to construct 3-dimensional circuits. If the vertical arm is very short, horizontal NWs on Si

substrates are grown. As can be observed in Fig. 4a, the NWs came out of a patterned

hole, with a good electrical contact with the substrate [62]. Then, the growth direction

switched ~90° and the growth continues along the horizontal direction. As can be seen

in Fig. 4b, these NWs are elongated along the <112> direction respect to the vertical

NW growth, which is similar to Fig. 1d and 3c. The surface of the horizontal segment

is very smooth, which could minimize the surface-roughness-induced carrier scattering.

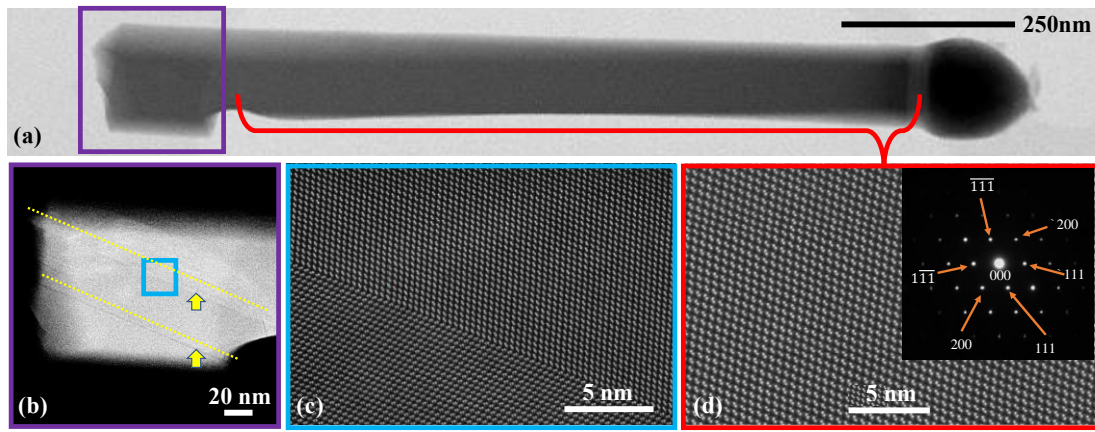*Structural properties of horizontal NWs*

Fig. 5. Crystal structure of the horizontal GaAs$_{0.8}$P$_{0.2}$ NWs. (a) The low magnification

image shows the entire NW. (b) Zoom-in TEM image of the blue area shown in (a). There are

only few twin faults shown in the area pointed by the yellow arrows. The yellow dot lines are

guiding to the eye about the twin defects extending across the entire NW diameter. (c)

Atomic-resolution STEM image of the area shown in purple square in (b), which is a single

twin. (d) Atomic-resolution TEM image of the horizontal arm, which is pure ZB. The inset is

the SAED pattern.

The crystal quality is an extremely important factor that controls the device

performance. Thus, the crystal quality of these horizontal NWs was checked by

(S)TEM. Fig. 5a and b show a short vertical arm of the NW. There are a few sparse single twins observed in the corner region (Fig. 5b and c). These twins are not in horizontal direction, which suggests that they were not generated during the growth of the vertical segment. They should be associated to the growth direction switch. As proposed by Uccelli *et al.* [63] the generation of single twins is an effective way to force the change of the NW growth direction without the generation of broken atomic bonds. Thus, through the generation of a few twins, the growth front of horizontal NW switched to its own <111> direction despite that it is pointing close to the <112> direction of the vertical segment. The <111> direction is the most energetically preferable for zinc blende NW growth. NWs grown in this direction tend to be bounded by low surface energy side facets, e.g. {110}, which is beneficial for minimize the parasitic sidewall growth [44]. Thus, the horizontal NWs shown here has greatly improved diameter uniformity along the axis. The NW has a small tape ratio, calculated by measuring the diameter difference between the tip and bottom, $(D_{bottom}-D_{tip})/D_{bottom}$, of of 7~20%. Besides, the Ga(Be) droplet with a lowered surface energy is beneficial for supressing the wurtzite nucleation [64,65]. Therefore, the horizontal NW has a pure ZB crystal structure without defects been observed from multi-NWs we have checked (Fig. 5d), except some stacking faults at the very tip of the vertical NW that could be generated by the partial particle solidification during cooling down process [26]. Due to the absence of stacking faults, it is surface is smooth, which is potentially important for low carrier scattering. These horizontal NWs are grown with the same self-catalyzed

mode as vertical ones. Thus, we would not expect major difference in electrical and optical properties between them.
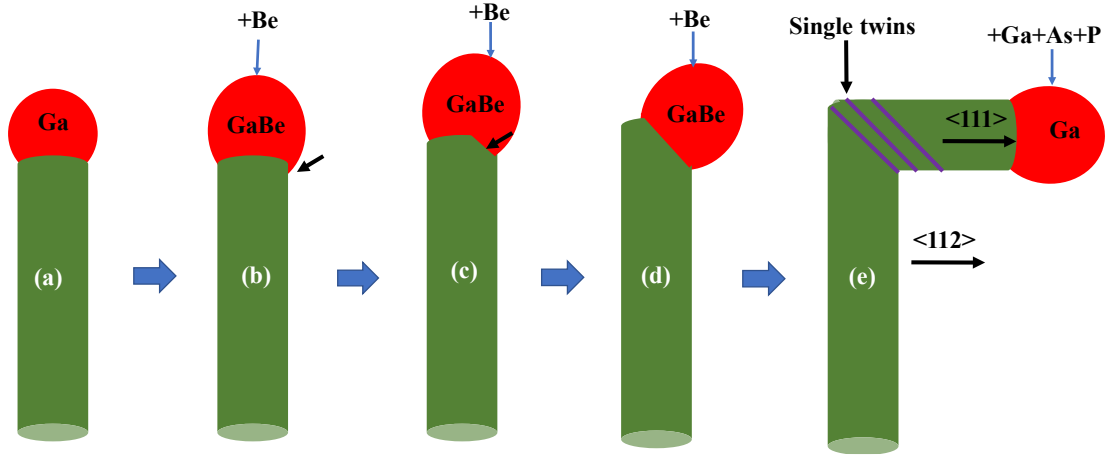

Fig. 6. illustration of the horizontal NW growth procedures. (a) Vertical growth. (b) Side wall setting at the location marked by a black arrow. (c) New facet development at the location marked by a black arrow. (d) Droplet slides off the top facet. (e) Growth front switch with the generation of single twins.

Conclusion

In summary, manipulation of self-catalytic droplet in GaAsP NWs to grow high-quality horizontal NWs is demonstrated and the procedures are illustrated in Fig. 6. Lowering the surface energy of Ga droplet (Fig. 6a) by the formation of Ga(Be) causes droplet sidewall setting (Fig. 6b), new facet generation (Fig. 6c) and in the end movement from the top to sidewalls of the NW (Fig. 6d). On the sidewalls, the droplet prefers to straddle <112> corner ridge and covers two of the six {110} facets, being more predominant in NWs with small diameters. After displacing from the tip, the droplet will stay at the NW tip and does not slide along the NW length, despite the

absence of stacking faults. This is can be explained from the lowered surface energy making the droplet wetting more efficient within the NW and "*holding*" it more tightly. For the generation of L-shape NWs, additional control to keep a low saturation level is required to avoid the droplet solidification. With the droplet on the sidewalls of a NW tip, a new equilibrium growth condition is required for the catalysed VLS growth to continue in a direction 90° relative to the initial NW axial direction. Through the generation of twins, the growth front switches the <111> direction to horizontal direction (Fig. 6e), which can grow NWs that tend to be bounded by low-surface energy facets. Thus, the parasitic shell growth is greatly supressed and the NWs can have a good diameter uniformity along the axis with a good and small tape ratio of 7~20%. Besides, the GaBe droplet with a lowered surface energy is beneficial for supressing the wurtzite nucleation, resulting NWs with a pure ZB crystal structure and smooth surface. These results lead to the first high-quality growth of self-catalysed horizontal NWs, which is an important step towards III-V NW-based large-scale integrated circuits and 3-dimensional circuits.

Experimental section

NW growth: The self-catalyzed GaAs NWs were grown directly on p-type Si substrates by means of solid-source III−V molecular beam epitaxy (MBE).[66] GaAs NWs were grown with a Ga beam equivalent pressure, V/III flux ratio, substrate temperature, growth duration and Be flux (equivalent to a nominal thin-film doping concentration) of 8.41×10^{-8} Torr, 44, ~630°C, 1 hour and $0\sim1.28\times10^{19}$/cm^3, respectively. The NWs grown on patterned Si substrates were performed with a

temperature of ~640°C, Ga flux of 1.6×10^{-7} Torr, V/III flux ratios between 3 and 20, and a P/(P+As) flux ratio of 12% throughout the growth duration of 45 minutes. The detailed information can be seen in Reference [62].

Scanning electron microscope (SEM): The NW morphology was measured with a Zeiss XB 1540 FIB/SEM system.

Transmission electron microscopy (TEM): Simple mechanical transfer of the NWs onto a lacey carbon support was used to prepare TEM specimens. The TEM measurements were performed using a doubly−corrected ARM200F microscope, operating at 200 kV.

ASSOCIATED CONTENT

Author Information:

Corresponding Author: Yunyan Zhang
*E-mail: yunyan.zhang.11@ucl.ac.uk

Declaration of Competing Interest:

The authors declare no competing financial interest.

Acknowledgements:

Reference

[1] C.M. Lieber, Z.L. Wang, MRS bulletin, 32 (2007) 99-108. https://doi.org/10.1557/mrs2007.41

[2] Y. Zhang, J. Wu, M. Aagesen, H. Liu, Journal of Physics D: Applied Physics, 48 (2015) 463001. https://doi.org/10.1088/0022-3727/48/46/463001

[3] R. Yan, D. Gargas, P. Yang, Nature photonics, 3 (2009) 569-576. https://doi.org/10.1038/nphoton.2009.184

[4] N.P. Dasgupta, J. Sun, C. Liu, S. Brittman, S.C. Andrews, J. Lim, H. Gao, R. Yan, P. Yang, Advanced materials, 26 (2014) 2137-2184. https://doi.org/10.1002/adma.201305929

[5] P. Yang, R. Yan, M. Fardy, Nano letters, 10 (2010) 1529-1536. https://doi.org/10.1021/nl100665r

[6] G. Zheng, F. Patolsky, Y. Cui, W.U. Wang, C.M. Lieber, Nature biotechnology, 23 (2005) 1294-1301. https://doi.org/10.1038/nbt1138

[7] Y. Huang, X. Duan, Y. Cui, L.J. Lauhon, K.-H. Kim, C.M. Lieber, Science, 294 (2001) 1313-1317. https://doi.org/10.1126/science.1066192

[8] S. De Franceschi, J. Van Dam, E. Bakkers, L. Feiner, L. Gurevich, L.P. Kouwenhoven, Applied Physics Letters, 83 (2003) 344-346. https://doi.org/10.1063/1.1590426

[9] Y.-J. Doh, J.A. van Dam, A.L. Roest, E.P. Bakkers, L.P. Kouwenhoven, S. De Franceschi, science, 309 (2005) 272-275. https://doi.org/10.1126/science.1113523

[10] M.S. Gudiksen, L.J. Lauhon, J. Wang, D.C. Smith, C.M. Lieber, Nature, 415 (2002) 617-620. https://doi.org/10.1038/415617a

[11] J.V. Holm, H.I. Jørgensen, P. Krogstrup, J. Nygård, H. Liu, M. Aagesen, Nature communications, 4 (2013) 1-5. https://doi.org/10.1038/ncomms2510

[12] M.H. Huang, S. Mao, H. Feick, H. Yan, Y. Wu, H. Kind, E. Weber, R. Russo, P. Yang, science, 292 (2001) 1897-1899. https://doi.org/10.1126/science.1060367

[13] J. Wu, A. Ramsay, A. Sanchez, Y. Zhang, D. Kim, F. Brossard, X. Hu, M. Benamara, M.E. Ware, Y.I. Mazur, Nano letters, 16 (2016) 504-511. https://doi.org/10.1021/acs.nanolett.5b04142

[14] O. Moutanabbir, S. Senz, R. Scholz, M. Alexe, Y. Kim, E. Pippel, Y. Wang, C. Wiethoff, T. Nabbefeld, F. Meyer zu Heringdorf, ACS nano, 5 (2011) 1313-1320. https://doi.org/10.1021/nn1030274

[15] J.J. Gu, X. Wang, H. Wu, J. Shao, A.T. Neal, M.J. Manfra, R.G. Gordon, P.D. Ye, 2012 International Electron Devices Meeting, IEEE2012, pp. 27.26. 21-27.26. 24. https://doi.org/10.1109/IEDM.2012.6479117

[16] F. Glas, Physical Review B, 74 (2006) 121302. https://doi.org/10.1103/PhysRevB.74.121302

[17] G. Cirlin, V. Dubrovskii, I. Soshnikov, N. Sibirev, Y.B. Samsonenko, A. Bouravleuv, J. Harmand, F. Glas, physica status solidi (RRL)–Rapid Research Letters, 3 (2009) 112-114. https://doi.org/10.1002/pssr.200903057

[18] T. Shimizu, T. Xie, J. Nishikawa, S. Shingubara, S. Senz, U. Gösele, Advanced Materials, 19 (2007) 917-920. https://doi.org/10.1002/adma.200700153

[19] M. Borg, H. Schmid, K.E. Moselund, G. Signorello, L. Gignac, J. Bruley, C. Breslin, P. Das Kanungo, P. Werner, H. Riel, Nano letters, 14 (2014) 1914-1920. https://pubs.acs.org/doi/pdf/10.1021/nl404743j

[20] U. Krishnamachari, M. Borgstrom, B. Ohlsson, N. Panev, L. Samuelson, W. Seifert,

M. Larsson, L. Wallenberg, Applied Physics Letters, 85 (2004) 2077-2079. https://doi.org/10.1063/1.1784548

[21] C. Zhang, X. Miao, P.K. Mohseni, W. Choi, X. Li, Nano letters, 14 (2014) 6836-6841. https://pubs.acs.org/doi/10.1021/nl502525z

[22] S.A. Fortuna, X. Li, IEEE Electron Device Letters, 30 (2009) 593-595. https://doi.org/10.1109/LED.2009.2019769

[23] A.W. Dey, C. Thelander, E. Lind, K.A. Dick, B.M. Borg, M. Borgstrom, P. Nilsson, L.-E. Wernersson, IEEE Electron Device Letters, 33 (2012) 791-793. https://doi.org/10.1109/LED.2012.2190132

[24] X. Miao, X. Li, IEEE electron device letters, 32 (2011) 1227-1229. https://doi.org/10.1109/LED.2011.2160248

[25] Y. Zhang, H.A. Fonseka, M. Aagesen, J.A. Gott, A.M. Sanchez, J. Wu, D. Kim, P. Jurczak, S. Huo, H. Liu, Nano letters, 17 (2017) 4946-4950. https://doi.org/10.1021/acs.nanolett.7b02063

[26] Y. Zhang, A.M. Sanchez, Y. Sun, J. Wu, M. Aagesen, S. Huo, D. Kim, P. Jurczak, X. Xu, H. Liu, Nano letters, 16 (2016) 1237-1243. https://doi.org/10.1021/acs.nanolett.5b04554

[27] Q. Li, S. Huang, D. Pan, J. Wang, J. Zhao, H. Xu, Applied Physics Letters, 105 (2014) 113106. https://doi.org/10.1063/1.4896105

[28] S.R. Plissard, I. Van Weperen, D. Car, M.A. Verheijen, G.W. Immink, J. Kammhuber, L.J. Cornelissen, D.B. Szombati, A. Geresdi, S.M. Frolov, Nature nanotechnology, 8 (2013) 859. https://www.nature.com/articles/nnano.2013.198

[29] P. Krogstrup, N. Ziino, W. Chang, S. Albrecht, M. Madsen, E. Johnson, J. Nygård, C.M. Marcus, T. Jespersen, Nature materials, 14 (2015) 400-406. https://www.nature.com/articles/nmat4176

[30] A. Kelrich, O. Sorias, Y. Calahorra, Y. Kauffmann, R. Gladstone, S. Cohen, M. Orenstein, D. Ritter, Nano letters, 16 (2016) 2837-2844. https://doi.org/10.1021/acs.nanolett.6b00648

[31] L. Li, D. Pan, X. Yu, H. So, J. Zhao, Journal of Semiconductors, 38 (2017) 103001. https://doi.org/10.1088/1674-4926/38/10/103001

[32] Y. Zi, K. Jung, D. Zakharov, C. Yang, Nano letters, 13 (2013) 2786-2791. https://doi.org/10.1021/nl4010332

[33] Y. Shen, R. Chen, X. Yu, Q. Wang, K.L. Jungjohann, S.A. Dayeh, T. Wu, Nano letters, 16 (2016) 4158-4165. https://doi.org/10.1021/acs.nanolett.6b01037

[34] W. Du, X. Yang, H. Pan, X. Ji, H. Ji, S. Luo, X. Zhang, Z. Wang, T. Yang, Nano letters, 16 (2016) 877-882. https://doi.org/10.1021/acs.nanolett.5b03587

[35] Y. Shen, S. Turner, P. Yang, G. Van Tendeloo, O.I. Lebedev, T. Wu, Nano letters, 14 (2014) 4342-4351. https://doi.org/10.1021/nl501163n

[36] X. Miao, C. Zhang, X. Li, Nano letters, 13 (2013) 2548-2552. https://doi.org/10.1021/nl400620f

[37] R. Dowdy, D.A. Walko, S.A. Fortuna, X. Li, IEEE Electron Device Letters, 33 (2012) 522-524. https://doi.org/10.1109/LED.2012.2186115

[38] R. Wagner, W. Ellis, Applied physics letters, 4 (1964) 89-90. https://doi.org/10.1063/1.1753975@apl.2019.APLCLASS2019.issue-1

[39] D. Tsivion, M. Schvartzman, R. Popovitz-Biro, P. von Huth, E. Joselevich, Science, 333 (2011) 1003-1007. https:// doi.org/10.1126/science.1208455

[40] S.A. Fortuna, J. Wen, I.S. Chun, X. Li, Nano Letters, 8 (2008) 4421-4427. https://doi.org/10.1021/nl802331m

[41] H.J. Joyce, Q. Gao, H.H. Tan, C. Jagadish, Y. Kim, X. Zhang, Y. Guo, J. Zou, Nano letters, 7 (2007) 921-926. https://doi.org/10.1021/nl062755v

[42] A. Rothman, V.G. Dubrovskii, E. Joselevich, Proceedings of the National Academy of Sciences, 117 (2020) 152-160. https://doi.org/10.1073/pnas.1911505116

[43] S. Breuer, C. Pfuller, T. Flissikowski, O. Brandt, H.T. Grahn, L. Geelhaar, H. Riechert, Nano letters, 11 (2011) 1276-1279. https://doi.org/10.1021/nl104316t

[44] D.E. Perea, J.E. Allen, S.J. May, B.W. Wessels, D.N. Seidman, L.J. Lauhon, Nano letters, 6 (2006) 181-185. https://doi.org/10.1021/nl051602p

[45] M. Bar-Sadan, J. Barthel, H. Shtrikman, L. Houben, Nano letters, 12 (2012) 2352-2356. https://doi.org/10.1021/nl300314k

[46] Y. Zhang, M. Aagesen, J.V. Holm, H.I. Jørgensen, J. Wu, H. Liu, Nano letters, 13 (2013) 3897-3902. https://doi.org/10.1021/nl401981u

[47] X. Yu, H. Wang, J. Lu, J. Zhao, J. Misuraca, P. Xiong, S. von Molnár, Nano letters, 12 (2012) 5436-5442. https://doi.org/10.1021/nl303323t

[48] L. Ghisalberti, H. Potts, M. Friedl, M. Zamani, L. Güniat, G. Tütüncüoglu, W.C. Carter, A.F. i Morral, Nanotechnology, 30 (2019) 285604. https://doi.org/10.1088/1361-6528/ab139c

[49] E.S. Koivusalo, T.V. Hakkarainen, H.V. Galeti, Y.G. Gobato, V.G. Dubrovskii, M.D. Guina, Nano letters, 19 (2018) 82-89. https://doi.org/10.1021/acs.nanolett.8b03365

[50] ADA COUNCIL ON SCIENTIFIC AFFAIRS, The Journal of the American Dental Association, 134 (2003) 476-478. https://doi.org/10.14219/jada.archive.2003.0198

[51] Y. Zhang, Z. Sun, A.M. Sanchez, M. Ramsteiner, M. Aagesen, J. Wu, D. Kim, P. Jurczak, S. Huo, L.J. Lauhon, Nano letters, 18 (2018) 81-87. https://doi.org/10.1021/acs.nanolett.7b03366

[52] T. Chow, Journal of Physics: Condensed Matter, 10 (1998) L445. https://doi.org/10.1088/0953-8984/10/27/001

[53] F. Glas, Journal of Applied Physics, 108 (2010) 073506. https://doi.org/10.1063/1.3488908

[54] Y. Zhang, A.M. Sanchez, J. Wu, M. Aagesen, J.V. Holm, R. Beanland, T. Ward, H. Liu, Nano letters, 15 (2015) 3128-3133. https://doi.org/10.1021/acs.nanolett.5b00188

[55] E. Uccelli, J. Arbiol, J.R. Morante, A. Fontcuberta i Morral, ACS nano, 4 (2010) 5985-5993. https://doi.org/10.1021/nn101604k

[56] M. Tornberg, K.A. Dick, S. Lehmann, Applied Physics Letters, 113 (2018) 123104. https://doi.org/10.1063/1.5045266

[57] F. Hejda, P. Solar, J. Kousal, Surface free energy determination by contact angle measurements–a comparison of various approaches. WDS2010, pp. 25-30.

[58] P. Sharma, K.H. Rao, Advances in colloid and interface science, 98 (2002) 341-463. https://doi.org/10.1016/S0001-8686(02)00004-0

[59] R. Gaskin, K. Steele, W. Forster, New Zealand Plant Protection, 58 (2005) 179-183. https://doi.org/10.30843/nzpp.2005.58.4244

[60] J. Nairn, W. Forster, New Zealand Plant Protection, 67 (2014) 278-283. https://doi.org/10.30843/nzpp.2014.67.5726

[61] V.G. Dubrovskii, G. Cirlin, N. Sibirev, F. Jabeen, J.-C. Harmand, P. Werner, Nano letters, 11 (2011) 1247-1253. https://doi.org/10.1021/nl104238d

[62] Y. Zhang, J. Wu, M. Aagesen, J. Holm, S. Hatch, M. Tang, S. Huo, H. Liu, Nano letters, 14 (2014) 4542-4547. https://doi.org/10.1021/nl501565b

[63] E. Uccelli, J. Arbiol, C. Magen, P. Krogstrup, E. Russo-Averchi, M. Heiss, G. Mugny, F. Morier-Genoud, J. Nygård, J.R. Morante, Nano letters, 11 (2011) 3827-3832. https://doi.org/10.1021/nl201902w

[64] E. Gil, V.G. Dubrovskii, G. Avit, Y. André, C. Leroux, K. Lekhal, J. Grecenkov, A. Trassoudaine, D. Castelluci, G. Monier, R.M. Ramdani, Nano letters, 14 (2014) 3938-3944. https://doi.org/10.1021/nl501239h

[65] D.L. Dheeraj, A.M. Munshi, M. Scheffler, A.T.J. Van Helvoort, H. Weman, B.O. Fimland, Nanotechnology, 24 (2012) 015601. https://doi.org/10.1088/0957-4484/24/1/015601

[66] Y. Zhang, A.M. Sanchez, M. Aagesen, S. Huo, H.A. Fonseka, J.A. Gott, D. Kim, X. Yu, X. Chen, J. Xu, Small, 15 (2019) 1803684. https://doi.org/10.1002/smll.201803684